International Journal of Pharmaceutics 423 (2012) 102–107

Contents lists available at ScienceDirect

International Journal of Pharmaceutics

journal homepage: www.elsevier.com/locate/ijpharm

Synthesis and functionalization of persistent luminescence nanoparticles with small molecules and evaluation of their targeting ability

Thomas Maldiney[a,b,c,d], Gerardo Byk[e], Nicolas Wattier[a,b,c,d], Johanne Seguin[a,b,c,d], Raz Khandadash[e], Michel Bessodes[a,b,c,d], Cyrille Richard[a,b,c,d,*], Daniel Scherman[a,b,c,d,**]

[a] Unité de Pharmacologie Chimique et Génétique et d'Imagerie, CNRS, UMR 8151, F-75270 Paris Cedex, France
[b] INSERM, U1022, F-75270 Paris Cedex, France
[c] Université Paris Descartes, Sorbonne Paris Cité, Faculté des Sciences Pharmaceutiques et Biologiques, Paris, F-75270 Cedex, France
[d] ENSCP, Chimie Paristech, F-75231 Paris Cedex, France
[e] Department of Chemistry, Laboratory of Nano-Biotechnology, and School of Engineering, Bar Ilan University, Ramat Gan 52900, Israel

ARTICLE INFO

Article history:
Received 10 June 2011
Accepted 29 June 2011
Available online 23 July 2011

Keywords:
Persistent luminescence nanoparticles
Surface functionalization
Binding
PC-3
In vitro

ABSTRACT

We have recently reported the design and use of inorganic nanoparticles with persistent luminescence properties. Such nanoparticles can be excited with a UV lamp for 2 min and emit light in the near-infrared area for dozen of minutes without any further excitation. This property is of particular interest for small animal optical imaging, since it avoids the autofluorescence of endogenous fluorophores which is one major problem encountered when using fluorescent probes. We report herein the synthesis of persistent luminescence nanoparticles (PLNPs) and their functionalization with two small targeting molecules: biotin and Rak-2. We provide characterization of each PLNP as well as preliminary evidence of the ability of PLNP-PEG-Biotin to target streptavidin and PLNP-PEG-Rak-2 to bind prostate cancer cells *in vitro*.

1. Introduction

Optical imaging techniques provide great potential for understanding biological processes at the molecular level and for sensitive cancer diagnosis, particularly at the early stage of cancer development (Bruchez et al., 1998). Biological optical imaging greatly relies upon the use of sensitive and stable optical labels. So far, organic dyes (Kogure et al., 2006), quantum dots (Chan and Nie, 1998; Gao et al., 2004; Michalet et al., 2005; Maysinger et al., 2007) and metal nanoparticles (Storhoff et al., 1998; Taton et al., 2000) are the most commonly used optical labels but still have some limitations. When used *in vivo*, fluorescent probes present numerous drawbacks (Ntziachristos, 2006) such as autofluorescence (Frangioni, 2003) coming from tissue organic components during probe illumination. In addition, deep tissue imaging is difficult because of critical absorption from major components present in living organism (water, melanin, haemoglobin, lipids).

To overcome these difficulties, we have recently developed inorganic persistent luminescence nanoparticles (PLNPs). The key element of this technology is based on long lasting luminescent nanoparticles which can be optically excited with a UV lamp before emitting in near-infrared range (le Masne de Chermont et al., 2007). The persistent luminescence is still detectable after 1 h. Among the different nanomaterials synthesized, we have shown that the composition $Ca_{0.2}Zn_{0.9}Mg_{0.9}Si_2O_6$ doped with luminescent ions (0.5% Eu^{2+}, 1% Dy^{3+} and 2.5% Mn^{2+}) was the best candidate for *in vivo* imaging (le Masne de Chermont et al., 2009). Neutral PLNP functionalized with a polyoxyethylene chain (PEG) could circulate in the blood for more than 30 min if injected i.v. 5 min after the preinjection of a negative liposome used the saturate the reticuloendothelial system (Kamps et al., 1999).

Malignant tumours display both increased angiogenesis and chaotic microenvironment growth, mainly responsible for hyper vascularization, leaky vasculature, and poor lymphatic drainage (Maeda et al., 2000; Brannon-Peppas and Blanchette, 2004). It has been reported that long-circulating nanoparticles with PEG modifications on their surface were able to favour passive tumour targeting (Moghimi et al., 2001; Greenwald, 2001). Injection of our PEG-PLNP to C57BL/6 mouse bearing an s.c. implanted Lewis lung carcinoma (3LL) tumour in the inguinal region, allowed us to detect the tumour vasculature during the first 2 min following the injection. However no passive accumulation of our PLNP-PEG could be observed at longer time. In order to favour a passive accumulation

* Corresponding author at: INSERM, U1022, CNRS, UMR 8151, Unité de Pharmacologie Chimique et Génétique et d'Imagerie, Faculté de Pharmacie, 4 avenue de l'Observatoire, 75006 Paris, France. Tel.: +33 1 53 73 95 67; fax: +33 1 43 26 69 18.
** Corresponding author at: INSERM, U1022, CNRS, UMR 8151, Unité de Pharmacologie Chimique et Génétique et d'Imagerie, Faculté de Pharmacie, 4 avenue de l'Observatoire, 75006 Paris, France.
E-mail addresses: cyrille.richard@parisdescartes.fr (C. Richard), daniel.scherman@parisdescartes.fr (D. Scherman).

0378-5173/$ – see front matter © 2011 Elsevier B.V. All rights reserved.
doi:10.1016/j.ijpharm.2011.06.048

of PEG-PLNP in the tumour area we recently reported the influence of both diameter of the PLNP (80, 120 and 180 nm) and length of the PEG chain (5, 10 and 20 kDa). This study revealed that 6 h after intravenous injection of 80 nm PLNP-$PEG_{10\,kDa}$ in 3LL tumour bearing mice, 5.9 ± 2.8% of the injected dose were located within the tumour micro-environment (Maldiney et al., 2011).

In the present article, we describe the first targeting strategies for the design and functionalization of persistent luminescent nanoparticles with small targeting molecules. The first example is based on the functionalization of PLNP with biotin in order to evaluate their binding affinity on streptavidin coated plate. The second example is based on the functionalization of PLNP with Rak-2, recently reported for its affinity toward PC-3 cells (Byk et al., 2010). This second molecule was taken as an example in this study, but the approach could be extended to other targeting moieties (Byrne et al., 2008; Loomis et al., 2011). Special attention was directed to provide full characterization of the probes through several analytical tools such as infrared spectrophotometry, thermogravimetric analysis, and classical physico-chemical measurements (zeta potential, dynamic light scattering) as well as colloidal stabilities. Finally we discussed preliminary targeting results of PLNP-PEG-Biotin on streptavidin coated plate and PLNP-PEG-Rak-2 on PC-3 cells *in vitro*.

2. Materials and methods

2.1. Materials

Inorganic salts (magnesium nitrate ($Mg(NO_3)_2$, $6H_2O$), zinc chloride ($ZnCl_2$), calcium chloride ($CaCl_2$, $2H_2O$), europium chloride ($EuCl_3$, $6H_2O$), dysprosium nitrate ($Dy(NO_3)_3$, $5H_2O$), manganese chloride ($MnCl_2$, $4H_2O$)), and tetraethoxysilane (TEOS), used for the synthesis of PLNP were purchased from Aldrich. 3-Aminopropyltriethoxysilane, diglycolic anhydride and propyl amine, NHS-PEG-Biotin were obtained from Sigma–Aldrich. BOP reagent (benzotriazole-1-yl-oxy-tris-pyrrolidino-phosphonium hexafluorophosphate) was purchased from Advanced ChemTech. Triethylamine (>99.5%) and dimethylformamide (>99.9%) were purchased from SDS. COOH-PEG-OMe was purchased from IrisBiotech. Streptavidin coated plate were obtained from Nunc®. Boc-21-amino-hexa oxa heneicosanoic acid (Boc-PEG-COOH) (code no. BA19206) was purchased from NeoMPS, Inc. High resolution p-ESI mass spectra were acquired with a ultra-high resolution mass spectrometer, the hybrid linear ion trap LTQ-Orbitrap (Thermo Fisher Scientific, Les Ulis, France). The analyses were performed using flow injection analysis (FIA) with Surveyor Autosampler and LC pump (Thermo Fisher Scientific). 20 μL of each sample (2 ng/μL of sample in MeOH solution) is injected in a continuous flow rate of MeOH at 100 μL/min. The electrospray voltage was set to 3.8 kV, the capillary voltage and the tube lens offset were set to 20 V and 70 V, respectively. The sheath gas flow (nitrogen) was optimized at 45 a.u. and the drying gas temperature was set to 275 °C. The mass resolving power (full width at half maximum height) was set at 6×10^4 FWHM.

2.2. Synthesis of PLNP

The PLNP were prepared using a procedure previously reported in our laboratory (le Masne de Chermont et al., 2009). Briefly, 126 mg of calcium chloride, 993 mg of magnesium nitrate, 527 mg of zinc chloride, 16 mg of europium chloride, 39 mg of dysprosium nitrate, 44 mg of manganese chloride, 4 mL of deionized water at pH 2 and 2 mL of TEOS were vigorously stirred at room temperature for 1 h and then warmed at 70 °C for 2 h (until the sol–gel transition occurred). The wet gel was then dried in an oven at 110 °C for 20 h to remove water and ethanol. The resulting opaque dry gel was then fired at 1050 °C for 10 h in a zircone crucible in a weak reductive atmosphere using 10% H_2, 90% Ar (Noxal 4, Air Liquide, Düsseldorf, Germany) to give white crystals.

2.3. Obtention of nanosized (80 and 180 nm) particles

Nanometer-sized particles were obtained by alcaline wet grinding of the solid (500 mg) for 15 min with a mortar and pestle in a minimum volume of 5 mM NaOH solution. Hydroxylation was then performed overnight by dispersing the ground powder in 50 mL of the same NaOH solution to get hydroxy-PLNP. Nanoparticles with a diameter of 180 nm were selected from the whole polydisperse colloidal suspension by centrifugation on a SANYO MSE Mistral 1000 at 4500 rpm for 5 min. They were located in the supernatant. The supernatants were gathered and concentrated to a final 5 mg/mL suspension. Nanoparticles with a diameter of 80 nm were obtained by centrifugation on a SANYO MSE Mistral 1000 at 4500 rpm for 30 min, the supernatant was concentrated from 50 mL to a final volume of 12 mL and a second centrifugation of the concentrated supernatant was realized on an Eppendorf MiniSpin Plus at 8000 rpm for 5 min. The resulting suspension was concentrated to a final amount of 5 mg/mL.

2.4. Synthesis of the small molecules

2.4.1. Boc-PEG-Rak-2

Trifluoroacetic acid (TFA) (1 mL) was added to a 5 mL round bottom flask containing 150 mg (0.32 mmol) of Rak-2 (synthesized as previously reported in Byk et al., 2010). The solution was stirred for 1 h at RT. Then, the TFA was removed under reduced pressure and the compound was dried in vacuum for 2 days. Then, 200 μL acetonitrile (CH_3CN) was added to the flask to dissolve the deprotected Rak-2 and a solution of Boc-$(PEG)_6$-OH (143 mg, 0.32 mmol) in 92 μL CH_3CN and BOP (155 mg, 0.352 mmol) were added. TEA (1.4 mmol, 200 μL) was added to the flask and the solution was stirred for 3 days. Then, CH_3CN was evaporated and the product was dried under vacuum to give a yellow oil. The residual oil was dissolved in 18 mL ethyl acetate and washed with water (10 mL 4×), 1 M $KHSO_4$ (5 mL 3×), 1 M $NaHCO_3$ (5 mL 3×), saturated NaCl (5 mL 3×) and dried over magnesium sulfate. The solvent was removed under vacuum. The obtained oil was dissolved in 5 mL MeOH and 140 mg Dowex 50 WX2-100 ion exchange resin (0.7 mmol/g) was added to the solution and stirred for 20 min to give 100 mg of pure product (40% yield). The product was fully analysed and deprotected with TFA for 1 h prior to conjugation to PLNPs. ^{1}H NMR (300 MHz, $CDCl_3$) δ 7.68 (s, 1H, H-3′), 7.42 (m, 1H, H-2′), 6.40 (bs, 1H, H-4′), 5.66 (s, 1H, H-14), 4.12 (m, 2H, H-12), 3.71 (t, 2H, H-18), 3.65 (m, 20H, H-19 to H-21), 3.53 (t, 2H, H-22), 3.31 (t, J = 5.1 Hz, 2H, H-23), 3.2 (m, 2H, H-5), 2.57 (t, J = 6 Hz, 2H, H-17), 1.86 (m, 2H, H-2), 1.62–1.68 (m, 4H, H-2 + H-3), 1.44 (s, 9H, H-26), 1.11–1.32 (m, 16H, H-5 to H-10, H-3 + H-2 + H-4), 0.85 (t, J = 7.2 Hz, 3H, H-11); ^{13}C NMR (50 MHz, $CDCl_3$) δ 171.78 (C-13), 168.90 (C-16), 167.861 (C-15), 156.03 (C-24), 143.36 (C-3′), 143.08 (C-2′), 118.98 (C-1′), 111.04 (C-4′), 70.54 (C-20), 70.39 (C-21, C-22), 70.20 (C-19), 67.04 (C-18), 55.24 (C-14), 48.58 (C-1), 46.11 (C-5), 41.62 (C-12), 40.50 (C-23), 36.47 (C-17), 28.41 (C-26), 22.47 (C-10), 14.01 (C-11), 32.74, 31.59, 29.35, 28.68, 26.77, 25.43, 24.71 (C-9, C-8, C-7, C-6, C-4, C-3, C-2). HRMS m/z calc. for $C_{41}H_{72}N_4O_{12}$ = 835.5039; found 835.507.

2.4.2. Boc-PEG-N-propyl amide

Boc-PEG-N-propyl amide was synthesized as Boc-PEG-Rak-2 but propylamine was used instead of deprotected Rak-2 as starting material. ^{1}H NMR (300 MHz, CDCl3) δ 6.54 (bs, 1H, H-4), 5.10 (bs, 1H, H-19), 3.72 (t, J = 4.2 Hz, 2H, H-17), 3.65 (m, 20H, H-7 to H-16), 3.54 (m, 2H, H-6), 3.31 (m, 2H, H-18), 3.21 (q, J = 5.1 Hz, 2H,

H-3), 2.47 (t, J = 4.2 Hz, 2H, H-5), 1.52 (sextet, J = 5.4 Hz, 2H, H-2), 1.44 (s, 9H, H-20), 0.91 (t, J = 5.4 Hz, 3H, H-1); HRMS m/z calc. for $C_{18}H_{39}O_7N_2$ = 395.2751; found 395.2760.

2.5. Surface modification

PLNP functionalized with Rak-2 and N-propyl amide (as negative control) were obtained from 80 or 180 nm hydroxy-PLNP. First, amino-PLNP were obtained from 200 mg of hydroxy-PLNP (80 or 180 nm), dispersed in 20 mL of dimethylformamide (DMF), to which 100 μL of 3-aminopropyl-triethoxysilane (APTES) was added under constant stirring. The suspension was then stirred overnight at room temperature. A series of centrifugation and redispersion in DMF were performed to wash the excess of APTES.

For binding assays on streptavidin plate, 4 mg of amino-PLNP (180 nm core) were reacted either with 100 mg of NHS-PEG-Biotin in 10 mL of DMSO or with 40 mg of COOH-PEG-OMe and 40 mg of BOP reagent in 2 mL of DMF. The suspensions were stirred for 10 h and the excess of reagent was removed by centrifugation.

For binding assays on PC-3 cells, carboxyl-PLNP were obtained starting from 20 mg of amino-PLNP redispersed in 7 mL of DMF to which diglycolic anhydride (5.4 mg, dissolved in 1 mL of DMF) were added. The suspension was stirred overnight at room temperature. Again, the excess of reactant was removed by the washing procedure. Finally, 19 mg of BOP dissolved in 2 mL of DMF were prepared and 400 μL of this solution added to 5 mg of carboxy-PLNP and 10 μmol of NH_2-$(PEG)_6$-Rak-2 or NH_2-$(PEG)_6$-N-propyl amide were added plus 5 μL of triethylamine. The mixture was stirred for 16 h and sonicated the first 2 h. The excess of reactant was removed by the washing procedure.

2.6. Characterization of functionalized PLNP

Each type of nanoparticles was characterized by different techniques. Dynamic light scattering and zeta potential measurements in 20 mM NaCl were performed on a Zetasizer Nano ZS (Malvern Instruments, Southborough, MA) equipped with a 632.8 nm helium neon laser and 5 mW power, with a detection angle at 173° (non-invasive back scattering). FT-IR spectra of PLNP-PEG-Rak-2 and PLNP-PEG-N-propyl amide were recorded on an Iraffinity-1 spectrophotometer from Shimadzu. Thermogravimetric analysis (TGA) was performed using a Setaram Setsys evolution 1600 (Argon atmosphere, temperature range: from 20 °C to 780 °C, 10 °C/min) on 10 mg of dry samples of 180 nm core PLNP, at each functionalization step. Briefly, for TGA analysis, the sample is gradually heated from 20 °C to 780 °C under argon atmosphere, and precision scales allow monitoring the weight loss as a function of temperature. Colloidal stabilities in DMEM culture medium of N-propyl amide or Rak-2 functionalized PLNP were determined by following the hydrodynamic diameter of the PLNP over 50 min after dispersion in DMEM.

2.7. Binding on streptavidin plate

To investigate the ability of the biotinylated PLNP to interact with streptavidin, we used a 96 wells Nunc® plate passively coated with streptavidin (Nunc A/S, Roskilde, Denmark). After being washed three times with a 0.05% PBS/Tween 20 solution, 100 μL of a 1 mg/mL suspension of nanoparticles dispersed in PBS, were deposited on the plate, incubated for 1 h at room temperature and washed three times to remove the unfixed nanoparticles. The amount of PLNP present on the plate was determined by luminescence detection using Wallac Victor^2 Multilabel Counter from Perkin Elmer (excitation filter: D355, emission filter: D615, counting delay: 1 ms, counting window: 5 ms, counting cycle: 6.1 ms).

Table 1
Zeta potential in 20 mM NaCl of the differently coated PLNP.

Nanoparticles	Zeta potential (mV)
Hydroxy-PLNP	−40
Amino-PLNP	+35
Carboxy-PLNP	−30
PLNP180-PEG-Rak-2	−16
PLNP180-PEG-N-propyl amide	−11
PLNP80-PEG-Rak-2	−13
PLNP80-PEG-N-propyl amide	−7

2.8. Cell culture

PC-3 cells, obtained from ATCC, were cultured in Nutrient Mixture Kaighn's Modification medium (F-12K) supplemented with 10% fetal calf serum, and antibiotics (100 μg/mL penicillin and 100 U/mL streptomycin). Cells were cultured at 37 °C in 5% CO_2 humidified atmosphere.

2.9. In vitro binding study to PC-3 cells

PC-3 cells were seeded in flat bottom 96-well at a density of 10^4 cells/well and grown overnight in 100 μL medium. For binding assay, each type of nanoparticle was incubated for either 15 or 30 min in complete DMEM culture medium. Cells were then washed three times with 10 mM PBS before luminescence detection using Wallac Victor^2 Multilabel Counter from Perkin Elmer (excitation filter: D355, emission filter: D615, counting delay: 1 ms, counting window: 5 ms, counting cycle: 6.1 ms).

3. Results and discussions

3.1. Synthesis of PLNP and functionalization with small molecules

Starting from 500 mg of crude PNLP, the hydroxylation process followed by centrifugation steps allowed us to isolate 10 mg (2% of total amount) of small (80 nm) hydroxy-$PLNP_{80}$ and 150 mg (30%) of larger (180 nm) hydroxy-$PLNP_{180}$ (Maldiney et al., 2011). These hydroxy-PLNP (80 and 180 nm) were reacted with APTES to give amino-PLNP. Then reaction were done either with NHS-PEG-Biotin or with COOH-PEG-OMe to give respectively PLNP-PEG-Biotin or PLNP-PEG (Scheme 1A). In parallel, reaction of amino-PLNP with diglycolic anhydride give carboxy-PLNP which reacted either with NH_2-PEG-Rak-2 or with NH_2-PEG-N-propyl amide to give respectively PLNP-PEG-Rak-2 or PLNP-PEG-propyl (Scheme 1B).

3.2. Characterization of the functionalized nanoparticles

3.2.1. Zeta potential

Each surface modification introduces molecules responsible for a characteristic global charge on the edge of the particles. Measurement of zeta potential (ZP) thus allows qualitative monitoring of all functionalization steps. Measurements were done using a Zetasizer Nano ZS from Malvern Instruments. As shown in Table 1, before any functionalization, hydroxy-PLNP display a net negative potential, attributed to the presence of silanol groups covering the probe. Amino-PLNP intermediate is characterized by a straight positive ZP due to amino groups on the surface which are protonated at physiological pH. The amino-PLNP were either functionalized by PEG-biotin (or PEG-OMe) for streptavidin binding assay, giving nanoparticles with ZP ~0 mV, or converted to carboxy-PLNP, with a global negative charge, attributed to the carboxylic acid functions. Grafting of PEG-N-propyl amide or PEG-Rak-2 on the surface of the particles led to a significant increase in ZP values, as compared to carboxy-PLNP, switching from highly negative ZP values (−30 mV) to a potential closer to neutrality (from −7 to −16 mV). This shift

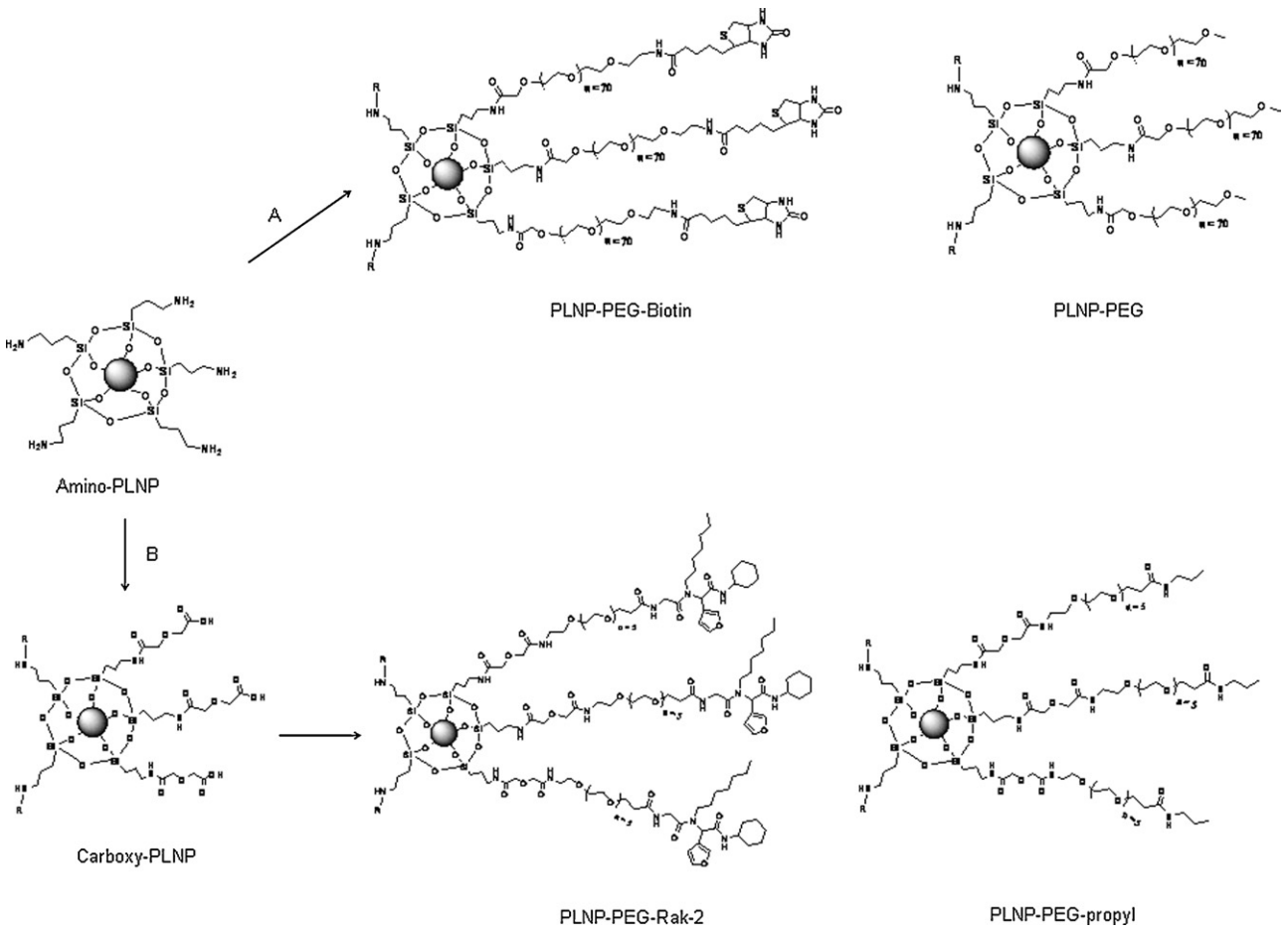

Scheme 1. Functionalization of PLNP. (A) NHS-PEG-Biotin, DMSO or COOH-PEG-OMe, DMF. (B) Diglycolic anhydride, DMF, then NH_2-PEG-N-propyl amide, BOP, TEA, DMF, overnight or NH_2-PEG-Rak-2, BOP, TEA, DMF, overnight.

can either be attributed to the disappearance of carboxyls which were transformed into amide bounds during the functionalization process with small molecules, or to the ligands PEG spacer, which partly masked the remaining carboxylic groups. Yet, we notice a little charge difference between N-propyl amide and Rak-2 functionalized PLNP. This deviation is certainly related to the remaining carboxyl groups on the surface of PLNP, which are fewer with N-propyl amide than with Rak-2. Indeed, given the large size of Rak-2 molecule as compared to N-propyl amide, steric hindrance is very likely to be responsible for this effect, limiting accessibility of the ligand to the surface of PLNP.

3.2.2. FT-IR spectra

FT-IR spectra of 180 nm PLNP after each step of the functionalization are presented in Fig. 1. Hydroxy-PLNP spectrum shows characteristic band of silicate powder at 1630 cm^{-1} (Fig. 1A). After reaction with APTES, the appearance of C–H stretch bands at 2940 cm^{-1} and at NH_2 bend at 1619 cm^{-1} (Fig. 1B) are characteristic of the presence of amine on silica nanoparticles (Shen et al., 2004). After reaction with diglycolic anhydride two characteristic peaks at 1640 cm^{-1} (amide bond) and 1425 cm^{-1} (CH_2COO) are visible in Fig. 1C. Finally, the introduction of PEG-Rak-2 molecule on PLNP was confirmed by the presence of new peaks at 1540 cm^{-1} (C–N bond) and 2933 cm^{-1} (CH_2 stretching, Fig. 1D), which are characteristic of the presence of the polyethylene glycol chain (Oh et al., 2009). Similar spectra were obtained with 80 nm PLNP.

3.2.3. Thermogravimetric analysis

Weight loss curves for 180 nm PLNP-PEG-Rak-2, as well as all intermediates, were obtained by thermogravimetric analysis (TGA) (Fig. 2). From amino-$PLNP_{180}$ to $PLNP_{180}$-PEG-Rak-2, we clearly distinguish two stages in surface decomposition. First, water trapped in the organic layer on the surface of PLNP evaporates before

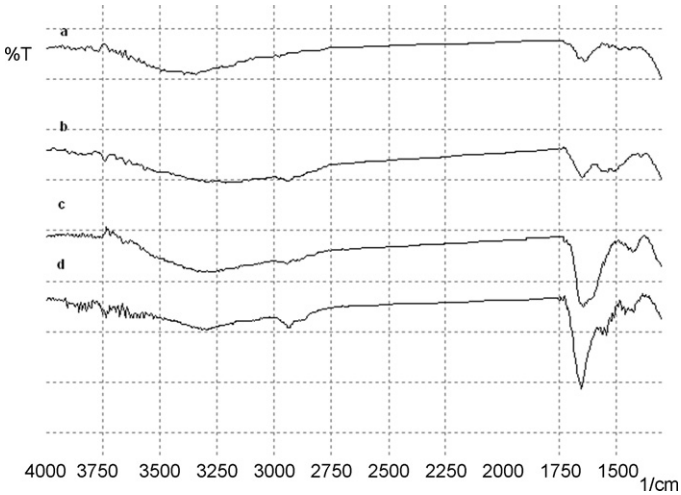

Fig. 1. FT-IR spectra of functionalized 180 nm PLNP. (A) Hydroxy-PLNP; (B) amino-PLNP; (C) carboxy-PLNP; (D) PLNP-PEG-Rak-2.

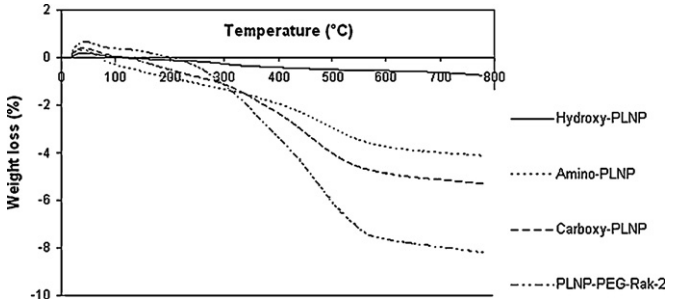

Fig. 2. Weight loss curves for 180 nm PLNP with different surface coverage.

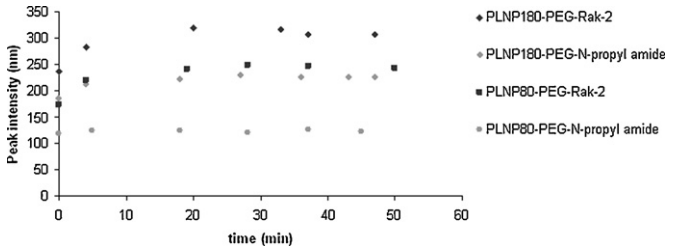

Fig. 3. Colloidal stabilities of 80 and 180 nm PLNP-PEG-Rak-2 and PLNP-PEG-N-propyl amide.

325 °C. The second stage begins after 325 °C and corresponds to the decomposition of organics present on the nanoparticles. Calculated values from weight loss percentage indicate that in the case of $PLNP_{180}$-PEG-Rak-2, the concentration of ligand on the surface of the nanoparticles reaches about 40 nmol/mg of PLNP. This value, which approximately corresponds to 70,000 Rak-2 molecules per nanoparticle, is consistent with our previous study on PEG-PLNP, in which we had shown that the higher the PEG molecular weight, the fewer chains remain on the surface (about 15 nmol/mg of PLNP for 5 kDa PEG) (Maldiney et al., 2011). In the case of PEG-Rak-2, the ligand molecular weight is about 7 times lighter than 5 kDa PEG, thus less affected by steric hindrance and more likely to gain access to nanoparticles surface. This is certainly the reason why we observe such a high value of Rak-2 ligand covalently linked to PLNP (40 nmol/mg) compared to heavier polymer chains.

3.3. Colloidal stability in assay medium

The colloidal stability of the 4 types of nanoparticles (80 and 180 nm PLNP-PEG-Rak-2 and PLNP-PEG-N-propyl amide) were studied in DMEM culture medium at 2 concentrations (300 and 600 μg/mL) for 50 min. Results concerning the concentration of 300 μg/mL are reported in Fig. 3. From this figure, we can deduce that the 4 types of PLNP are stable in culture medium for at least 50 min. No important increase of the size of each PLNP could be noticed. We also observe that the PLNP functionalized with the Rak-2 molecule (black spots in Fig. 3) always stabilized at a size higher than PLNP functionalized with N-propyl amide (grey spots). The hydrophobic nature of the Rak-2, as compared to N-propyl amide, could be responsible for this difference. However in all cases, stable suspensions of nanoparticles were obtained, which is a prerequisite for *in vitro* assays. Similar results are obtained at 600 μg/mL (data not shown).

Table 2
Binding study on streptavidin coated plate. The intensity of luminescence in arbitral unit (a.u.) after 60 min binding is dependent of the amount of PLNP retained on the plate.

Nanoparticles	Intensity (a.u.)
PLNP-PEG	2000
PLNP-PEG-Biotin	13,000
Biotinylated antibody + PLNP-PEG-Biotin	2000

3.4. Binding assay on streptavidin plate

Two types of nanoparticles have been prepared: PLNP-PEG and PLNP-PEG-Biotin, dispersed in PBS at a concentration of 1 mg/mL. These nanoparticles (100 μL) were deposited on a streptavidin plate, incubated for 30 min and washed. The quantity of PLNP retained on the streptavidin plate was determined using time-resolved fluorescence. As can be seen in Table 2, the immobilization of the PLNP on the plate is dependent of the presence of biotin: no immobilization occurred with PLNP-PEG, which is coherent with previous results (Longo and Szleifer, 2005). Moreover, we have shown that the immobilization of the PLNP was specific to biotin since a dramatic decrease of PLNP immobilized on the plate was observed when the plate was first incubated with biotinylated antibodies, which saturate the biotin binding site of immobilized streptavidin.

3.5. In vitro assays on PC-3 cells

In vitro binding assays were performed on the human prostate cancer PC-3 cell line which has been shown to specifically bind the Rak-2 molecule (Byk et al., 2010). Fig. 4 reports the intensity of PLNP luminescence detected after a 30 min incubation of PLNP on PC-3 cells. Experiments were conducted with either Rak-

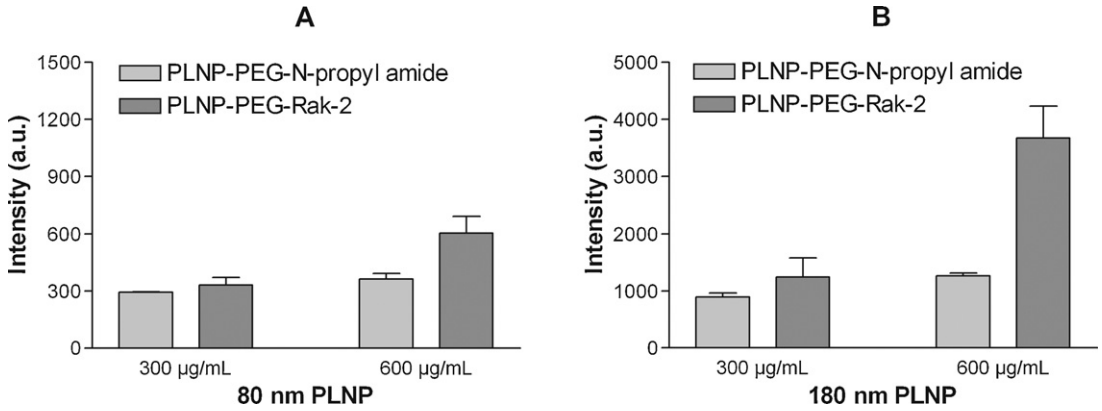

Fig. 4. *In vitro* binding study on PC-3 cells. (A) 80 nm PLNP; (B) 180 nm PLNP. Histograms represent the intensity of luminescence in arbitral unit (a.u.) after 30 min binding of PLNP on malignant cells.

2 or N-propyl amide-covered PLNP, with different core diameters (80 and 180 nm), and at two concentrations (300 and 600 μg/mL). The amount of PLNP retained on the cell layer highly depends on both the concentration of the suspension and the nature of the molecules grafted on the surface. Results in Fig. 4A show that at the highest concentration (600 μg/mL), large Rak-2-covered PLNP (180 nm core diameter) bind about 2.9 times more efficiently than non targeted PLNP. A weaker but similar trend is observed with 80 nm PLNP (Fig. 4B), where Rak-2 signal appears only 1.5 times brighter than the negative control. This size-dependent efficiency gap between 80 nm and 180 nm PLNP could either be the result of a combined gravitational-targeting effect (Gentile et al., 2008), which is naturally increased for larger particles (more likely to drift toward cell layer). Alternatively, this difference could be related to an avidity effect as a 180 nm nanoparticle would probably display more available Rak-2 ligands to bind PC-3 cell than smaller 80 nm PLNP (Hong et al., 2007; Simnick et al., 2010). This first binding study provides interesting preliminary results on the ability of Rak-2 functionalized PLNP to target PC-3 cells. However, additional work is needed, especially control binding on other cell lines (prostate non-cancer primary cells, for example), in order to ensure that such preferential binding on PC-3 cells is really specific to the presence of Rak-2 on the nanoparticles.

4. Conclusion

We have successfully synthesized and functionalized an original bioimaging probe, based on persistent luminescence nanoparticles, with two small targeting molecules: biotin and Rak-2. The latter was shown to be highly stable in complete DMEM culture medium, no matter how large the core diameter or high the concentration of the suspension. Pursuing the idea that such functionalized nanoparticles could be used as future sensitive optical probes for cancer imaging, we reported preliminary results showing immobilization of PLNP-PEG-Biotin on streptavidin plate and binding of PLNP-PEG-Rak-2 on prostate cancer cells.

Acknowledgements

This work has been supported by the French National Agency (ANR) in the frame of its program in Nanosciences and Nanotechnologies (NATLURIM project no. ANR-08-NANO-025) and by the Region Ile-de-France (In Actio project no. I07-876/R). G. Byk is indebted to the Israel-USA Binational Science Foundation (BSF 1998378) and to the AFIRST Israel/France (programs of the French Ministry of Foreign Affairs and the Israeli Ministry of Sciences). R. Khandadash would like to express his sincere gratitude to the Israel Council for Higher Education for waiving the Converging Technologies Fellowship, to BIU President Scholarships for waiving fellowship and to the Marcus Center for Medicinal Chemistry for their continuous support.

References

Brannon-Peppas, L., Blanchette, J.O., 2004. Nanoparticle and targeted systems for cancer therapy. Adv. Drug Deliv. Rev. 56, 1649–1659.

Bruchez, M.J., Moronne, M., Gin, P., Weiss, S., Alivisatos, A.P., 1998. Semiconductor nanocrystals as fluorescent biological labels. Science 281, 2013–2016.

Byk, G., Partouche, S., Weiss, A., Margel, S., Khandadash, S., 2010. Fully synthetic phage-like system for screening mixtures of small molecules in live cells. J. Comb. Chem. 12, 332–345.

Byrne, J.D., Betancourt, T., Brannon-Peppas, L., 2008. Active targeting schemes for nanoparticle systems in cancer therapeutics. Adv. Drug Deliv. Rev. 60, 1615–1626.

Chan, W.C.W., Nie, S., 1998. Quantum dot bioconjugates for ultrasensitive nonisotopic detection. Science 281, 1016–1018.

Frangioni, J.V., 2003. In vivo near-infrared fluorescence imaging. Curr. Opin. Chem. Biol. 7, 626–634.

Gao, X., Cui, Y., Levenson, R.M., Chung, L.W.K., Nie, S., 2004. In vivo cancer targeting and imaging with semiconductor quantum dots. Nat. Biotechnol. 22, 969–976.

Gentile, F., Curcio, A., Indolfi, C., Ferrari, M., Decuzzi, P., 2008. The margination propensity of spherical particles for vascular targeting in the microcirculation. J. Nanobiotechnol. 6, 1–9.

Greenwald, R.B., 2001. PEG drug: an overview. J. Controlled Release 74, 159–171.

Hong, S., Leroueil, P.R., Majaros, I.J., Orr, B.G., Baker, J.R., Banaszak Holl, M.M., 2007. The binding avidity of a nanoparticle-based multivalent targeted drug delivery platform. Chem. Biol. 14, 107–115.

Kamps, J.A., Morselt, H.W.M., Scherphof, G.L., 1999. Uptake of liposomes containing phosphatidylserine by liver cells *in vivo* and by sinusoidal liver cells in primary culture: *in vivo–in vitro* differences. Biochem. Biophys. Res. Commun. 256, 57–62.

Kogure, T., Karasawa, S., Araki, T., Saito, K., Kinjo, M., Miyawaki, A., 2006. A fluorescent variant of a protein from the stony coral *Montipora* facilitates dual-color single-laser fluorescence cross-correlation spectroscopy. Nat. Biotechnol. 24, 577–581.

le Masne de Chermont, Q., Chanéac, C., Seguin, J., Pelle, F., Maîtrejean, S., Jolivet, J.-P., Gourier, D., Bessodes, M., Scherman, D., 2007. Nanoprobes with near-infrared persistent luminescence for *in vivo* imaging. Proc. Natl. Acad. Sci. U. S. A. 104, 9266–9271.

le Masne de Chermont, Q., Richard, C., Seguin, J., Chanéac, C., Bessodes, M., Scherman, D., 2009. Silicates doped with luminescent ions: useful tools for optical imaging applications. Proc. of SPIE 7189, 71890B/1–71890B/9.

Longo, G., Szleifer, I., 2005. Ligand–receptor interactions in tethered polymer layers. Langmuir 21, 11342–11351.

Loomis, K., McNeeley, K., Bellamkonda, R.V., 2011. Nanoparticles with targeting, triggered release, and imaging functionality for cancer applications. Soft Matter 7, 839–856.

Maeda, H., Wu, J., Sawa, T., Matsumura, Y., Hori, K., 2000. Tumor vascular permeability and the EPR effect in macromolecular therapeutics: a review. J. Controlled Release 65, 271–284.

Maldiney, T., Richard, C., Seguin, J., Wattier, N., Bessodes, M., Scherman, D., 2011. Effect of core diameter, surface coating and PEG chain length on the biodistribution of persistent luminescent nanoparticles in mice. ACS Nano 5, 854–862.

Maysinger, D., Behrendt, M., Lalancette-Hebert, M., Kriz, J., 2007. Real-time imaging of astrocyte response to quantum dots: *in vivo* screening model system for biocompatibility of nanoparticles. Nano Lett. 7, 2513–2520.

Michalet, X., Pinaud, F.F., Bentolila, L.A., Tsay, J.M., Doose, S., Li, J.J., Sundaresan, G., Wu, A.M., Gambhir, S.S., Weiss, S., 2005. Quantum dots for live cells, in vivo imaging, and diagnostics. Science 307, 538–544.

Moghimi, S.M., Hunter, C., Murray, J.C., 2001. Long-circulating and target-specific nanoparticles: theory to practice. Pharmacol. Rev. 53, 283–318.

Ntziachristos, V., 2006. Fluorescence molecular imaging. Annu. Rev. Biomed. Eng. 8, 1–33.

Oh, C., Lee, Y.-G., Choi, T.-S., Jon, C.-U., Oh, S.-G., 2009. Facile synthesis of PEG-silica hybrid particles using one-step sol-gel reaction in aqueous solution. Colloids Surf. A: Physicochem. Eng. Asp. 349, 145–150.

Simnick, A.J., Valencia, C.A., Liu, R., Chilkoti, A., 2010. Morphing low-affinity ligands into high-avidity nanoparticles by thermally triggered self-assembly of a genetically encoded polymer. ACS Nano 4, 2217–2227.

Shen, G., Horgan, A., Levicky, R., 2004. Reaction of N-phenyl maleimide with aminosilane monolayers. Colloids Surf. B: Biointerfaces 35, 59–65.

Storhoff, J.J, Elghanian, R., Mucic, R.C., Mirkin, C.A., Letsinger, R.L., 1998. One-pot colorimetric differentiation of polynucleotides with single base imperfections using gold nanoparticle probes. J. Am. Chem. Soc. 120, 1959–1964.

Taton, T.A., Mirkin, C.A., Letsinger, R.L., 2000. Scanometric DNA array detection with nanoparticle probes. Science 289, 1757–1760.